Revision 1

1   # Local peralkalinity in peraluminous granitic pegmatites. I. Evidence

2   # from whewellite and hydrogen carbonate in fluid inclusions

3   **YONGCHAO LIU[1,2], CHRISTIAN SCHMIDT[2,*], AND JIANKANG LI[1]**

4   [1]MNR Key Laboratory of Metallogeny and Mineral Assessment, Institute of Mineral Resources,

5   Chinese Academy of Geological Sciences, Beijing 100037, China

6   [2]GFZ German Research Centre for Geosciences, Telegrafenberg, 14473 Potsdam, Germany

7   *Corresponding author: Christian.Schmidt@gfz-potsdam.de

8

9   **ABSTRACT**

10   Fluid inclusions in pegmatite minerals were studied using Raman spectroscopy to

11   determine the carbon species. Carbon dioxide is very abundant in the aqueous liquid and vapor

12   phases. Occasionally, CH_4 was found in the vapor. In the aqueous liquid, HCO_3^- was detected in

13   fluid inclusions in tantalite-(Mn) from the Morrua Mine and in late-stage quartz from the Muiâne

14   pegmatite and the Naipa Mine, all in the Alto Ligonha District, Mozambique. Moreover, we

15   observed a carbonate (calcite group) in fluid inclusions in garnet from the Naipa Mine and in

16   beryl from the Morrua Mine, both in the Alto Ligonha District, Mozambique, and a calcite-group

17   carbonate and whewellite $[CaC_2O_4 \cdot H_2O]$ in fluid inclusions in topaz from Khoroshiv, Ukraine.

18   The occurrence of oxalate is interpreted to be due to a reaction of some form of carbon (possibly

19   CO or bitumen) with a peralkaline fluid. The results of our study support the hypothesis that,

20   although counterintuitive, hydrogen carbonate-rich peralkaline fluids may locally be involved in

21   the evolution of peraluminous granitic pegmatites, in which peralkaline minerals are normally

22   absent or very rare.

23   **Keywords:** whewellite, carbonate, hydrogen carbonate, oxalate, CO_2, fluid inclusion, pegmatite

24

INTRODUCTION

26   Carbon species are of particular interest in geochemistry and petrology because their

27   study can provide information on formation conditions. With exception of the ubiquitous carbon

28   dioxide, they are rare in peraluminous granitic pegmatites. Fluid inclusions with nahcolite

29   [$NaHCO_3$] and zabuyelite [Li_2CO_3] crystals in addition to aqueous carbonate/bicarbonate-rich

30   solution and CO_2 have been reported to occur in graphic granite of simple pegmatites from the

31   Klippeløkken granite quarry, east of Rønne, Bornholm Island, Denmark (Thomas et al. 2011) and

32   in pegmatitic granites from the Marcação, Galo Branco, and Picuí quarries, in the Borborema

33   Pegmatite Province, NE-Brazil (Beurlen et al. 2014). Similarly, crystal-rich inclusions containing

34   zabuyelite, calcite, pollucite-analcime, quartz/cristobalite, albite, and cookeite were found in

35   spodumene from the Tanco, Jiajika, Muiâne, Bikita, Kamativi, Lacorne, Zhawulong and other

36   pegmatites (London 1986; Anderson et al. 2001; Lima et al. 2003; Thomas and Davidson 2010;

37   Li and Chou 2016, 2017; Mulja and Williams-Jones 2018; Xiong et al. 2019). Macroscopic

38   primary carbonates (calcite, rhodochrosite, siderite, cerussite (maybe secondary), calcioancylite-

39   (Ce), bastnaesite-(Ce), synchisite-(Ce), parisite-(Ce), and even zabuyelite) and carbonate-rich

40   fluorapatite are generally very rare in peraluminous granitic pegmatites but there are several

41   reports from well-studied localities, e.g. the Bennett, Berry-Havey, Dunton, Emmons, Mount

42   Mica, and other pegmatites in Maine, USA, the Palermo No. 1 and No. 2 Mines, New

43   Hampshire, USA, the Foote Mine, North Carolina, USA, the Tanco Mine, Manitoba, Canada

44   (www.mindat.org), and the Khoroshiv (Volyn) pegmatites, Ukraine (Lyckberg et al. 2009).

45   Vuggy masses of Mn and Fe carbonate occur in the core zone of the Mount Mica pegmatite

46   (Simmons et al. 2016). London (2013) noted the occurrence of carbonates (calcite or

47 rhodochrosite) in "pocket" assemblages of granitic pegmatites. Alkali carbonate/bicarbonate-

48 bearing fluid inclusions in graphic granite and pegmatitic granite have been interpreted to

49 indicate the existence of peralkaline fluids early in the pegmatite evolution (Thomas et al. 2006a,

50 2011; Beurlen et al. 2014), although peraluminous phases crystallize until the latest stages. On

51 the other hand, it has been argued that zabuyelite, cristobalite, and cookeite in crystal-rich fluid

52 inclusions in spodumene were formed by a late-stage subsolidus reaction of spodumene with the

53 entrapped CO_2-rich aqueous fluid (Anderson et al. 2001; Anderson 2013, 2019). Such a reaction

54 appears to have occurred in the case of quartz-hosted primary fluid inclusion containing

55 spodumene, calcite, and rossmanite [$LiAl_8Si_6O_{18}(BO_3)_3(OH)_4$] from the Lacorne spodumene

56 pegmatite (Mulja and Williams-Jones 2018).

57   Carbonates in peraluminous granitic pegmatites can be viewed as oddities, and their

58 origin is still unclear. Even stranger appears to be the sporadic occurrence of kerite in "pockets"

59 with beryl and topaz in pegmatites at Khoroshiv (Volodarsk-Volynskii), Ukraine (Lyckberg et al.

60 2009). Because carbon species can provide information about formation conditions, we studied

61 fluid inclusions with carbon-bearing phases in pegmatite minerals from the Alto Ligonha region,

62 Mozambique (von Knorring and Condliffe 1987; Dias and Wilson 2000), the Khoroshiv District,

63 Ukraine (Lyckberg et al. 2009) and the Erongo region, Namibia (Cairncross and Bahmann 2006)

64 using Raman spectroscopy.

65

66   **EXPERIMENTAL METHODS**

67   Doubly polished sections were prepared from quartz, beryl, elbaite, tantalite-(Mn),

68 almandine-spessartine, albite, and K-feldspar from four pegmatites (Muiâne, Morrua, Naipa,

69 Nuaparra) in the Alto Ligonha region, Mozambique (e.g. Schmidt 1986; von Knorring and

70   Condliffe 1987; Schmidt and Thomas 1990a, 1990b; Dias and Wilson 2000). In addition, we

71   studied fluid inclusions in topaz from a pegmatite in the Khoroshiv District, Ukraine (Lyckberg

72   et al. 2009) and from a miarolitic cavity in the Klein Spitzkoppe granite, Namibia (Cairncross

73   2005) and in fluorite from the Hohenstein area, Erongo, Namibia (Cairncross and Bahmann

74   2006). Raman spectra of phases in these inclusions and of the host mineral were recorded using a

75   HORIBA Jobin Yvon LabRAM HR800 Vis Raman spectrometer equipped with a Synapse® 2048

76   × 512 back-illuminated CCD-detector, a Laser Quantum Torus 532 DPSS laser for excitation at

77   532.17 nm, a grating of 1800 lines/mm, a confocal pinhole diameter of 100 mm, and an Olympus

78   50× SLMPlan N objective (numerical aperture 0.35). The spectra were acquired with 4

79   accumulations of 20 s each.

80

81   **RESULTS**

82   The results of the Raman spectroscopic analyses of these inclusions are summarized in

83   Table 1. Aqueous inclusions were found in all studied late-stage ("pocket") minerals. In most

84   samples, CO_2 was observed in both the vapor and the aqueous liquid phases. Methane and

85   nitrogen were detected in the vapor phase of fluid inclusions in topaz from Khoroshiv and in

86   fluorite from Hohenstein/Erongo, and additionally hydrogen in the latter. A common solute in

87   the aqueous liquid was $[B(OH)_3]^0$, but HCO_3^- (aq) was not rare and detected in fluid inclusions in

88   tantalite-(Mn) from the Morrua Mine and in late-stage quartz from the Muiâne pegmatite and the

89   Naipa and Nuaparra Mines of the Alto Ligonha District, Mozambique (Figs. 1a and 1b).

90   Dissolved sulfate was only detected in fluid inclusions in the quartz sample 83391 from the

91   Naipa Mine (Table 1). Observed carbon-bearing solids included a calcite-group mineral (the

92   wavenumbers of the Raman bands suggest a $(Mn,Ca,Fe)CO_3$ solid solution) in fluid inclusions in

93   garnet from the Naipa Mine (Figs. 1c and 2), in beryl from the Morrua Mine (Figs. 3 and 4), and

94   in topaz from Khoroshiv (Fig. 5a). Surprisingly, whewellite [$CaC_2O_4 \cdot H_2O$] was identified in

95   fluid inclusions in topaz from Khoroshiv, Ukraine (Figs. 5b and 6). Whewellite shows

96   characteristic intense Raman bands (Fig. 6) at about 1462, 1489, and 1629 cm^{-1} (Duval and

97   Condrate Sr. 1988). Other identified solids were quartz, mica group mineral(s), bertrandite,

98   fluorapatite, triplite, herderite, hambergite, berborite, sassolite, elpasolite, and (tentatively)

99   saltonseaite (Table 1).

100

101   **DISCUSSION**

102   Our inclusion study supports the hypothesis of a possible local presence of peralkaline

103   fluid during crystallization of a peraluminous granitic pegmatite. Firstly, hydrogen carbonate was

104   detected in the aqueous solutions of fluid inclusions in tantalite-(Mn) from the Morrua Mine and

105   quartz from the Muiâne pegmatite and the Naipa Mine. Secondly, whewellite was found in fluid

106   inclusions in the topaz from the Khoroshiv (Volodarsk) District (Figs. 5b and 6). Whewellite is

107   known from numerous hydrothermal carbonate-sulfide veins or in sedimentary rocks and is

108   thought to form by oxidation of organic material. To our knowledge, an oxalate has not

109   previously been reported from a peraluminous granitic pegmatite. However, the pegmatites in the

110   Khoroshiv District, Ukraine, may be a peculiar case because a mineral related to organic matter

111   and a tar-like organic compound have been reported (buddingtonite and "kerite") (Lyckberg et al.

112   2009). It is important for the interpretation to bear in mind that alkali carbonate, oxalate, and

113   other abiogenic C-bearing species occur in alkaline igneous rock complexes (Nivin et al. 2005).

114   The presence of bitumen, oxalate minerals (natroxalate and whewellite), carboxylate compounds,

115   and kyanoxalite (a silicate with an oxalate group) is confirmed for late stages of the formation of
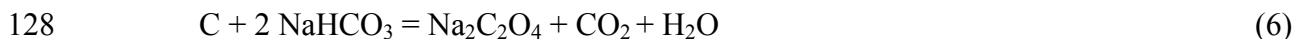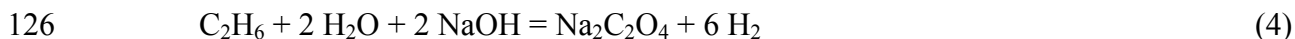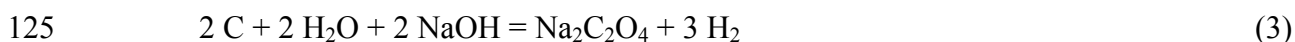
116   hyperalkaline pegmatites in the Lovozero alkaline pluton, Kola Peninsula, Russia (Chukanov et

117   al. 2010). The oxalates are thought to have formed at reducing and peralkaline conditions

118     $$2\,CO + 2\,NaOH = 2\,NaCOOH = Na_2C_2O_4 + H_2 \qquad (1)$$

119   (Chukanov et al. 2010). This mechanism of sodium oxalate formation from carbon monoxide via

120   formate was already described by Boswell and Dickson (1918). Sodium oxalate then reacts with

121   Ca in aqueous solution to form whewellite, e.g.

122     $$Na_2C_2O_4 + Ca^{2+} + H_2O = CaC_2O_4{\cdot}H_2O + 2\,Na^+ \qquad (2)$$
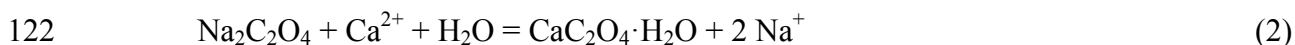
123   Conceivably, other reactions involving carbonaceous substances and peralkaline fluid may also

124   have caused oxalate formation

125     $$2\,C + 2\,H_2O + 2\,NaOH = Na_2C_2O_4 + 3\,H_2 \qquad (3)$$

126     $$C_2H_6 + 2\,H_2O + 2\,NaOH = Na_2C_2O_4 + 6\,H_2 \qquad (4)$$

127     $$C + H_2O + Na_2CO_3 = Na_2C_2O_4 + H_2 \qquad (5)$$

128     $$C + 2\,NaHCO_3 = Na_2C_2O_4 + CO_2 + H_2O \qquad (6)$$

129   Although reactions (3) to (6) are speculative, this is not the case for equations (1) and (2).

130   Thus, we interpret the origin of whewellite in fluid inclusions in topaz from the Khoroshiv

131   District to be due to a reaction of some form of reduced carbon (possibly CO or organic matter)

132   with a peralkaline fluid during crystallization of a nominally peraluminous granitic pegmatite.

133   Daughter crystals of a calcite-group carbonate were fairly common and were identified in

134   different pegmatite minerals, i.e. almandine-spessartine from the Naipa Mine, beryl from the

135   Morrua Mine, and topaz from the Khoroshiv (Volodarsk) District (Figs. 1c, 3, and 5a). However,

136   such carbonates do not necessarily indicate peralkaline conditions. The species HCO_3^-(aq)

137   predominates over CO_3^{2-}(aq) at elevated temperatures in aqueous fluids (Schmidt 2014), and

138   thus carbonate and CO_2 can form upon cooling by the inverse recombination reaction of the

139   hydrogen carbonate autoprotolysis (Rudolph et al. 2008)

140        $HCO_3^-(aq) + HCO_3^-(aq) = CO_3^{2-}(aq) + CO_2 + H_2O$ (7)
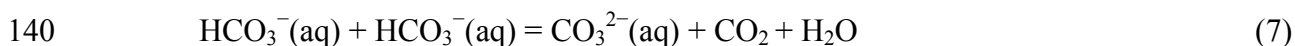
141   In our study, we found evidence for peralkaline fluids in pegmatites with Li

142   mineralization (petalite, spodumene, polylithionite-trilithionite, or amblygonite), i.e. in the

143   Khoroshiv (Volodarsk-Volynskii) District and in the Alto Ligonha District (Naipa and Morrua

144   Mines and the Muiâne and Nuaparra pegmatites), but not in the miarolitic pegmatites in the

145   Erongo region (Klein Spitzkoppe and Hohenstein) which do not contain spodumene or petalite.

146   This is due to the small sample size and does not imply a relationship of peralkaline fluids and

147   lithium mineralization. Carbonates and hydrogen carbonates (including zabuyelite, nahcolite,

148   dawsonite, calcite) have not only been reported to occur in fluid inclusions from numerous

149   spodumene-bearing pegmatites (Williams and Taylor 1996; Anderson 2001; Lima et al. 2003;

150   Sirbescu and Nabelek 2003; Thomas et al. 2006a; Beurlen et al. 2014; Li and Chou 2016, 2017;

151   Mulja and Williams-Jones 2018; Xiong et al. 2019), but also from rather simple pegmatites, e.g.

152   at Ehrenfriedersdorf, Saxony, Germany (Rickers et al. 2006), at Rønne, Bornholm Island,

153   Denmark (Thomas et al. 2011), and in the Königshain granite, Oberlausitz, Germany (Thomas

154   and Davidson 2016).

155   Thomas et al. (2006a) argue that alkali carbonates and hydrogen carbonate in granitic

156   pegmatites result from reaction of an alkali silicate melt with CO_2. In the case of the Jiajika

157   pegmatite, Li and Chou (2017) and Ding et al. (2020) suggested that the minerals within the

158   spodumene-hosted inclusions represent daughter minerals crystallized from an entrapped

159   carbonate- and silica-rich medium. London (2015) attributed the formation of carbonate to

160   enrichment in boundary layers generated during rapid growth of large crystals, and pointed out

161   that the composition of such fluid inclusions is very often not representative due to

162   heterogeneous trapping. Anderson (2019) proposed that the reaction of spodumene with CO_2 and

163   H_2O from a secondary infiltrating fluid (Anderson 2013) to zabuyelite, quartz or cristobalite, and

164   cookeite

165         $$5\ LiAlSi_2O_6 + 2\ CO_2 + 4\ H_2O = 2\ Li_2CO_3 + 7\ SiO_2 + LiAl_4(Si_3Al)O_{10}(OH)_8 \qquad (8)$$

166   accounts for the formation of the spodumene-hosted lithium carbonate-bearing inclusions in the

167   Tanco pegmatite. Segeler et al. (1981) and Nizamoff (2006) reported the occurrence of

168   carbonate-hydroxylapatite in the Palermo No. 1 and No. 2 pegmatites, New Hampshire, USA

169   that was interpreted to be the product of autometasomatic alteration of primary phosphates by

170   carbonate-bearing aqueous fluids. In this context, we note that carbonate-rich fluorapatite occurs

171   in both peraluminous granitic pegmatites (e.g. the Foote Mine in North Carolina, or the Dunton,

172   Bennett, Emmons and Mount Mica Mines in Maine, or the Etta Mine in South Dakota) and

173   alkaline rocks (e.g. Mont Saint-Hilaire, Ilimaussaq, Langesundsfjord, Kovdor, Khibiny,

174   Lovozero), just to name some famous localities (www.mindat.org). In summary, the occurrence

175   of whewellite is not the only indication that peralkaline fluids (in the broader sense including

176   melts) can locally occur during formation of peraluminous granitic pegmatites.

177

178   **IMPLICATIONS**

179   Our find of whewellite in fluid inclusions in topaz from the Khoroshiv District points to

180   reaction of reduced carbonaceous material with an alkaline fluid. The occurrence of alkali

181   carbonate and hydrogen carbonate does also indicate the presence of alkaline melts and/or

182   alkaline aqueous fluids in peraluminous granitic pegmatites. However, different opinions exist on

183   the origin of such alkaline conditions. Thomas et al. (2006b) attribute the formation of

184   peralkaline melt fractions to fractional crystallization and melt-melt immiscibility in

185   peraluminous granites and granite-related pegmatites. Experiments show that immiscibility

186   phenomena are enhanced in peralkaline silicic systems and by the presence of CO_3^{2-} (Veksler

187   2004) but unmixing of a peralkaline melt from a peraluminous silicic melt has not been observed

188   in the expected range of bulk flux concentrations of pegmatite-forming peraluminous granitic

189   melts (London 2015). The pegmatite model proposed by London (2009) involves the formation

190   of a flux-rich, potentially peralkaline, hydrosilicate liquid boundary layer that forms along the

191   crystallization front. London (2015) points out that carbonate in inclusions in pegmatite minerals

192   may result from heterogeneous trapping, and that the bulk composition of what is crystallizing in

193   a peraluminous pegmatite remains peraluminous even in late stages of its evolution (as manifest

194   in early almandine and biotite, later muscovite and polylithionite-trilithionite, and late "pocket"

195   clay minerals). This implies that development of peralkaline conditions can only occur on a

196   small, local, scale in such a pegmatite. On this scale, both opinions are not in conflict. With

197   respect to carbonates in inclusions, we conclude that non-alkali carbonates in peraluminous

198   pegmatites should not be interpreted as indicators of alkaline conditions.

199

207 support from the National Key R&D program of China (2019YFC0605200), the National

208 Natural Science Foundation of China (41872096), and the Chinese National Non-profit Institute

209 Research Grant of CAGS-IMR (JYYWF201814).

210

211 **REFERENCES CITED**

212 Anderson, A.J. (2013) Are silicate-rich inclusions in spodumene crystallized aliquots of

213   boundary layer melt? Geofluids, 13, 460−466.

214 Anderson, A.J. (2019) Microthermometric behavior of crystal-rich inclusions in spodumene

215   under confining pressure. Canadian Mineralogist, 57, 853−865.

216 Anderson, A.J., Clark, A.H., and Gray, S. (2001) The occurrence and origin of zabuyelite

217   (Li_2CO_3) in spodumene-hosted fluid inclusions: Implications for the internal evolution of

218   rare-element granitic pegmatites. Canadian Mineralogist, 39, 1513−1527.

219 Beurlen, H., Thomas, R., Rodrigues da Silva, M.R., Müller, A., Rhede, D., and Soares, D.R.

220   (2014) Perspectives for Li- and Ta-mineralization in the Borborema Pegmatite Province,

221   NE-Brazil: A review. Journal of South American Earth Sciences, 56, 110−127.

222 Boswell, M.A., and Dickson, J.V. (1918) The action of sodium hydroxide on carbon monoxide,

223   sodium formate and sodium oxalate. Journal of the American Chemical Society, 40,

224   1779−1786.

225 Cairncross, B. (2005) Famous mineral localities: Klein Spitzkoppe, Namibia. The Mineralogical

226   Record, 36, 317−335.

227 Cairncross, B., and Bahmann, U. (2006) Famous mineral localities: The Erongo Mountains

228   Namibia. The Mineralogical Record, 37, 361−470.

229   Chukanov, N.V., Pekov, I.V., Olysych, L.V., Massa, W., Yakubovich, O.V., Zadov, A.E.,

230   Rastsvetaeva, R.K., and Vigasina, M.F. (2010) Kyanoxalite, a new cancrinite-group mineral

231   species with extraframework oxalate anion from the Lovozero alkaline pluton, Kola

232   Peninsula. Geology of Ore Deposits, 52, 778−790.

233   Dias, M.B., and Wilson, W.E. (2000) The Alto Ligonha pegmatites: Mozambique. The

234   Mineralogical Record, 31, 459−497.

235   Ding, X., Li, J.K., Chou, I-M., Chen, Z.Y., and Li, S.H. (2020) Raman spectroscopic

236   identification of cookeite in the crystal-rich inclusions in spodumene from the Jiajika lithium

237   pegmatite deposit, China, and its geological implications. European Journal of Mineralogy,

238   32, 67−75.

239   Duval, D., and Condrate Sr., R.A. (1988) A Raman spectral study of the dehydration of calcium

240   oxalate monohydrate. Applied Spectroscopy, 42, 701−703.

241   Li, J.K., and Chou, I-M. (2016) An occurrence of metastable cristobalite in spodumene-hosted

242   crystal-rich inclusions from Jiajika pegmatite deposit, China. Journal of Geochemical

243   Exploration, 171, 29−36.

244   Li, J.K., and Chou, I-M. (2017) Homogenization experiments of crystal-rich inclusions in

245   spodumene from Jiajika lithium deposit, china, under elevated external pressures in a

246   hydrothermal diamond-anvil cell. Geofluids, 2017, 1−12.

247   Lima, A.M.C., Martins, T.C., Vieira, R.C., and Noronha, F. (2003) The study of fluid inclusions

248   in petalite-bearing pegmatite-aplite veins of the Barroso-Ãlvao field (Northern Portugal).

249   Acta Mineralogica-Petrographica, Abstract Series 2, 111−112.

250   London, D. (1986) Magmatic-hydrothermal transition in the Tanco rare-element pegmatite:

251   Evidence from fluid inclusions and phase-equilibrium experiments. American Mineralogist,

252   71, 376−395.

253   London, D. (2009) The origin of primary textures in granitic pegmatites. Canadian Mineralogist,

254   47, 697−724.

255   London, D. (2013) Crystal-filled cavities in granitic pegmatites: bursting the bubble. Rocks &

256   Minerals, 88, 527−538.

257   London, D. (2015) Reply to Thomas and Davidson on "A petrologic assessment of internal

258   zonation in granitic pegmatites" (London, 2014a). Lithos, 212−215, 469−484.

259   Lyckberg, P., Chornousenko, V., and Wilson, W.E. (2009) Famous mineral localities: Volodarsk-

260   Volynski, Zhitomir Oblast, Ukraine. The Mineralogical Record, 40, 473−506.

261   Mulja, T., and Williams-Jones, A.E. (2018) The physical and chemical evolution of fluids in rare-

262   element granitic pegmatites associated with the Lacorne pluton, Québec, Canada. Chemical

263   Geology, 493, 281−297.

264   Nivin, V.A., Treloar, P.J., Konopleva, N.G., and Ikorsky, S.V. (2005) A review of the occurrence,

265   form and origin of C-bearing species in the Khibiny Alkaline Igneous Complex, Kola

266   Peninsula, NW Russia. Lithos, 85, 93−112.

267   Nizamoff, J. (2006) The mineralogy, geochemistry & phosphate paragenesis of the Palermo #2

268   pegmatite, north Groton, New Hampshire, 149 p. M.S. thesis, University of New Orleans.

269   Rickers, K., Thomas, R., and Heinrich, W. (2006) The behavior of trace elements during the

270   chemical evolution of the H_2O-, B-, and F-rich granite–pegmatite–hydrothermal system at

271   Ehrenfriedersdorf, Germany: a SXRF study of melt and fluid inclusions. Mineralium

272   Deposita, 41, 229−245.

273   Rudolph, W.W., Irmer, G., and Koenigsberger, E. (2008) Speciation studies in aqueous HCO_3^-–

274   CO_3^{2-} solutions. A combined Raman spectroscopic and thermodynamic study. Dalton

275   Transactions 8, 900-8.

276   Schmidt, W. (1986) Geologische Entwicklung und Lagerstättenbi dung der Pegmatitregion von

277   Alto Ligonha, VR Moçambique. Dissertation B, Mining Academy Freiberg.

278   Schmidt, C. (2014) Raman spectroscopic determination of carbon speciation and quartz

279   solubility in H_2O + Na_2CO_3 and H_2O + $NaHCO_3$ fluids to 600 °C and 1.53 GPa. Geochimica

280   et Cosmochimica Acta, 145, 281−296.

281   Schmidt, W., and Thomas, R. (1990a) Zur Genesis von Seltenmetall-Granitpegmatiten auf der

282   Grundlage von Einschlußuntersuchungen und geochemischen Betrachtungen. Zeitschrift für

283   geologische Wissenschaften, 18, 301−314.

284   Schmidt, W., and Thomas, R. (1990b) Scheme of the genesis of Nb-Ta-pegmatites outlined by

285   the study of inclusions. Zeitschrift für geologische Wissenschaften, 18, 443−446.

286   Segeler, C.G., Kampf, A.R., Ulrich, W., and Whitmore, R.W. (1981) Phosphate minerals of the

287   Palermo No. 1 Pegmatite. Rock & Minerals, 56, 197−214.

288   Simmons, W., Falster, A., Webber, K., Roda-Robles, E., Boudreaux, A., Grassi, L.R., and

289   Freeman, G. (2016) Bulk composition of the Mt. Mica pegmatite, Maine, USA: Implications

290   for the origin of an LCT type pegmatite by anatexis. Canadian Mineralogist, 54, 1053−1070.

291   Sirbescu, M.-L.C., and Nabelek, P.I. (2003) Dawsonite: An inclusion mineral in quartz from the

292   Tin Mountain pegmatite, Black Hills, South Dakota. American Mineralogist, 88,

293   1055−1060.

294   Thomas, R., and Davidson, P. (2010) Hambergite-rich melt inclusions in morganite crystals from

295   the Muiane pegmatite, Mozambique and some remarks on the paragenesis of hambergite.

296   Mineralogy and Petrology, 100, 227−239.

297   Thomas, R., and Davidson, P. (2016) Origin of miarolitic pegmatites in the Königshain

298   granite/Lusatia. Lithos, 260, 225−241.

299   Thomas, R., Webster, J.D., and Davidson, P. (2006a) Understanding pegmatite formation: The

300   melt and fluid inclusion approach. Mineralogical Association Canada Short Course, 36,

301   189−210.

302   Thomas, R., Webster, J.D., Rhede, D., Seifert, W., Rickers, K., Förster, H.-J., Heinrich, W., and

303   Davidson, P. (2006b) The transition from peraluminous to peralkaline granitic melts:

304   Evidence from melt inclusions and accessory minerals. Lithos, 91, 137−149.

305   Thomas, R., Davidson, P., and Schmidt, C. (2011) Extreme alkali bicarbonate- and carbonate-

306   rich fluid inclusions in granite pegmatite from the Precambrian Rønne granite, Bornholm

307   Island, Denmark. Contributions to Mineralogy and Petrology, 161, 315−329.

308   Veksler, I.V. (2004) Liquid immiscibility and its role at the magmatic−hydrothermal transition: a

309   summary of experimental studies. Chemical Geology, 210, 7−31.

310   von Knorring, O., and Condliffe, E. (1987) Mineralized pegmatites in Africa. Geological Journal,

311   22, 253−270.

312   Williams, A.E., and Taylor, M.C. (1996) Mass spectrometric identification of boric acid in fluid

313   inclusions in pegmatite minerals. Geochimica et Cosmochimica Acta, 60, 3435−3443.

314   Xiong, X., Li, J.K., Wang, D.H., Li, S.P., and Lin, H. (2019) Fluid characteristics and evolution

315   of the Zhawulong granitic pegmatite lithium deposit in the Ganzi-Songpan region,

316   Southwestern China. Acta Geologica Sinica (English Edition), 93, 943−954.

317

318   **Figure captions**

319

320   Figure 1. Fluid inclusions in tantalite-(Mn) (**a**), quartz (**b**), and almandine-spessartine (**c**) from

321   pegmatites in the Alto Ligonha region, Mozambique (Morrua Mine (**a**), Muiâne pegmatite (**b**),

322   Naipa Mine (**c**)). Cg calcite group mineral, Ui unidentified mineral with Raman bands at 668 and

323   539 cm^{-1}, L aqueous liquid, V vapor.

324

325   Figure 2. Raman spectra of calcite group mineral in the fluid inclusion in almandine-spessartine

326   shown in Fig. 1c (left) and the almandine-spessartine host near that inclusion.

327

328   Figure 3. Fluid inclusions in beryl from the Morrua Mine, Mozambique. Cg calcite group

329   mineral, Brt bertrandite, CO_2-L CO_2-rich liquid, CO_2-V CO_2-rich vapor, L aqueous liquid, V

330   vapor.

331

332   Figure 4. Raman spectra of the beryl host and of solid phases in fluid inclusions in beryl from the

333   Morrua Mine, Mozambique.

334

335   Figure 5. Fluid inclusions in topaz from one pegmatite in the Khoroshiv District, Ukraine. Cg

336   calcite group mineral, L aqueous liquid, V vapor.

337

338   Figure 6. Raman spectra of whewellite and aqueous liquid in the fluid inclusion in topaz shown

339   in Fig. 5b and the topaz host near that inclusion.

340

341   Table 1. Results of the Raman spectroscopic analyses of fluid inclusions in pegmatite minerals.

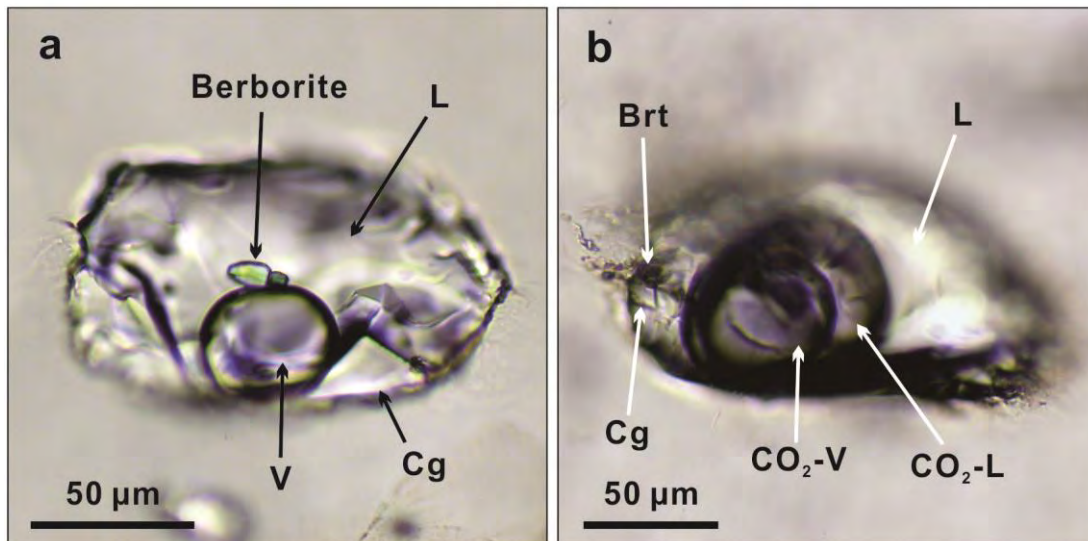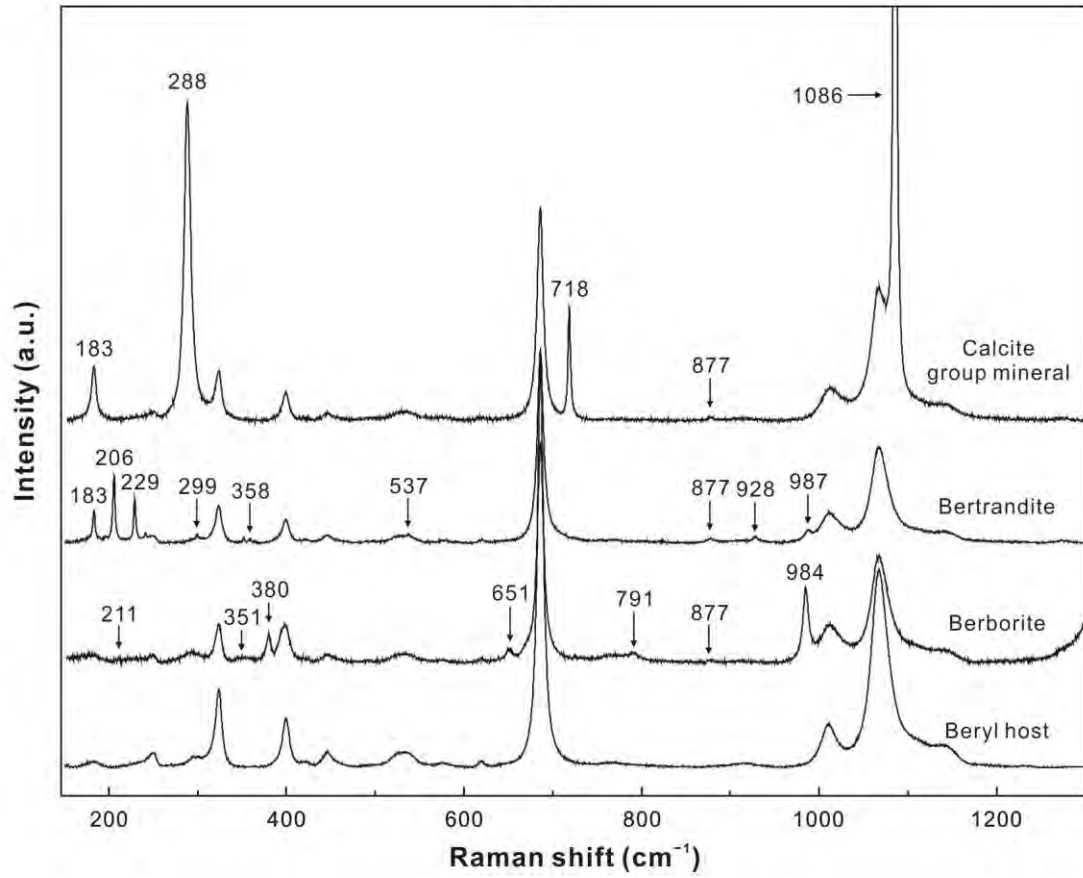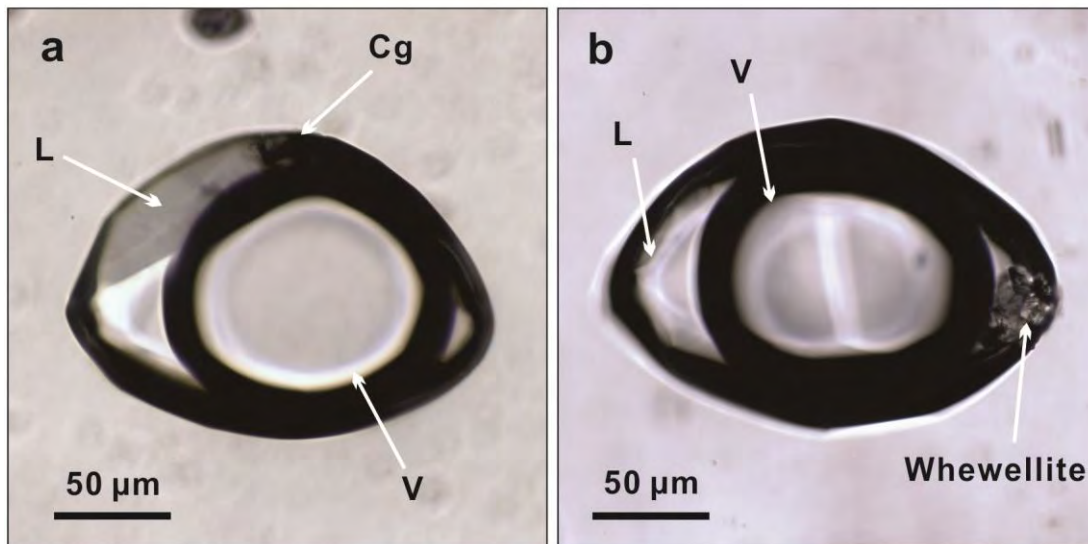| Sample	Vapor	Aqueous Liquid	Solid phases	Notes
Albite var. Cleavelandite 8/81/9, Naipa Mine, Mozambique	CO_2	CO_2, $[B(OH)_3]^0$		unidentified solid(s) with bands at 256, 355, 371, 402, 453, 747, 994, 1050, 1122, and 1137 cm^{-1}
K-feldspar Nai2 (=8/81/8), Naipa Mine, Mozambique	CO_2	CO_2, $[B(OH)_3]^0$		doubly terminated skeletal crystal
Almandine-Spessartine Nai 1 (=8/81/1), Naipa Mine, Mozambique			calcite group mineral, quartz, mica group mineral	unidentified mineral with bands at 668 and 539 cm^{-1}
Quartz 83391 (=8/81/7), Naipa Mine, Mozambique	CO_2	CO_2, HCO_3^-, $[B(OH)_3]^0$, SO_4^{2-}		doubly terminated crystal
Beryl, colorless, 36/5, Morrua Mine, Mozambique	CO_2	CO_2, $[B(OH)_3]^0$	calcite group mineral, bertrandite, berborite	
Tantalite-(Mn) Mor1, Morrua Mine, Mozambique	CO_2	CO_2, HCO_3^-		HCO_3^- signal weak (I_{1017}=~35/60 sec)
Beryl, pale blue, Mui1/2 (=12/81/x), Muiâne pegmatite, Mozambique	CO_2		mica group mineral	
Elbaite, yellowish green, Mui2/1 (=12/81/x), Muiâne pegmatite, Mozambique	CO_2	CO_2, $[B(OH)_3]^0$	fluorapatite, sassolite	
Elbaite, dark green, Mui2/2 (=12/81/x), Muiâne pegmatite, Mozambique	CO_2	CO_2, $[B(OH)_3]^0$	quartz	
Elbaite, pink, Mui2/3 (=12/81/x), Muiâne pegmatite, Mozambique	CO_2	CO_2, $[B(OH)_3]^0$	quartz	unidentified mineral with strong band at 518 cm^{-1}, additional unidentified solids
Quartz 83442 (=6/81/1), Muiâne pegmatite, Mozambique	CO_2	CO_2, HCO_3^-, $[B(OH)_3]^0$		the fluid inclusion shown in Fig. 1b is from sample 83442
Quartz 83386 (=13/81/9A), Nuaparra pegmatite, Mozambique	CO_2	CO_2, HCO_3^-		
Fluorite ,Hohenstein area, Erongo, Namibia			saltonseaite? (bands at 167, 236, ~692 cm^{-1})	fluid inclusions in central green zone: solids common, most of them without Raman bands. Unidentified solids with bands at 185, 197, 385, 642, 648 cm^{-1} and at 198, 328, 541, 570, 681 cm^{-1}
Fluorite, Hohenstein area, Erongo, Namibia	CO_2, N_2, CH_4, H_2	CO_2, $[B(OH)_3]^0$		outer colorless zone: no solids observed in the fluid inclusions
Topaz SK1, Klein Spitzkoppe, Namibia	CO_2	$[B(OH)_3]^0$	quartz, triplite	other, unidentified, minerals
Topaz 62/365, Khoroshiv (Volodarsk-Volynskii), Ukraine	CO_2, N_2, CH_4	CO_2, $[B(OH)_3]^0$	whewellite, calcite group mineral, elpasolite, herderite, hambergite, mica group mineral	other, unidentified, minerals

342

Fig. 1

2
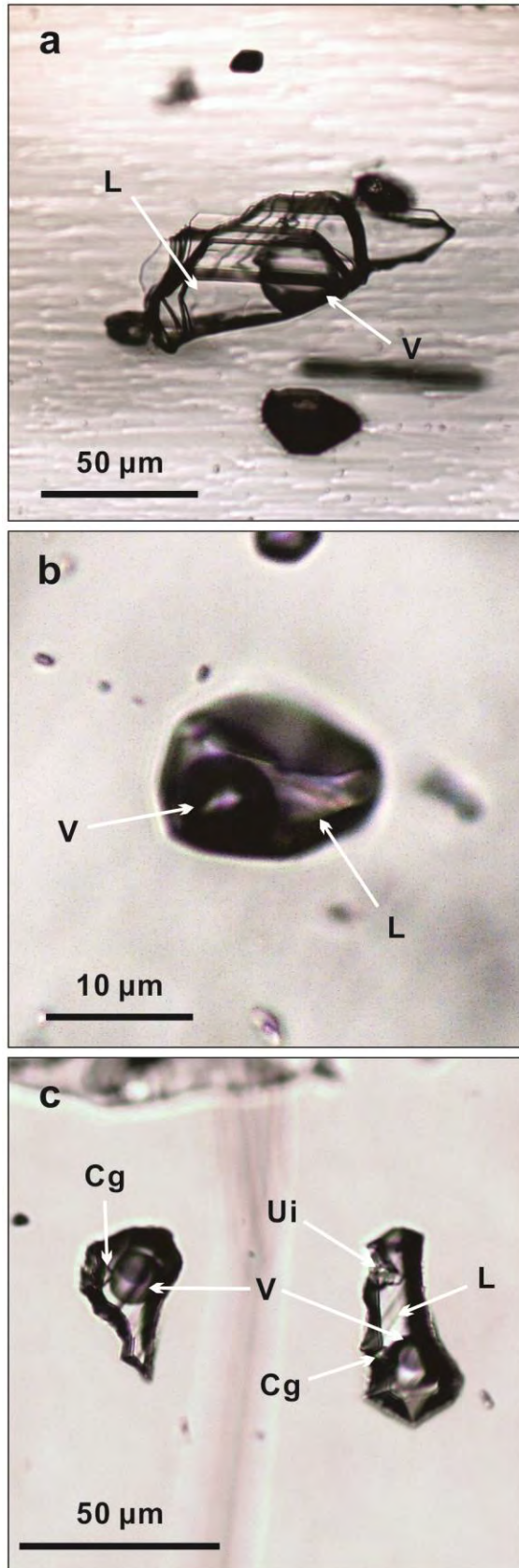
Fig. 2
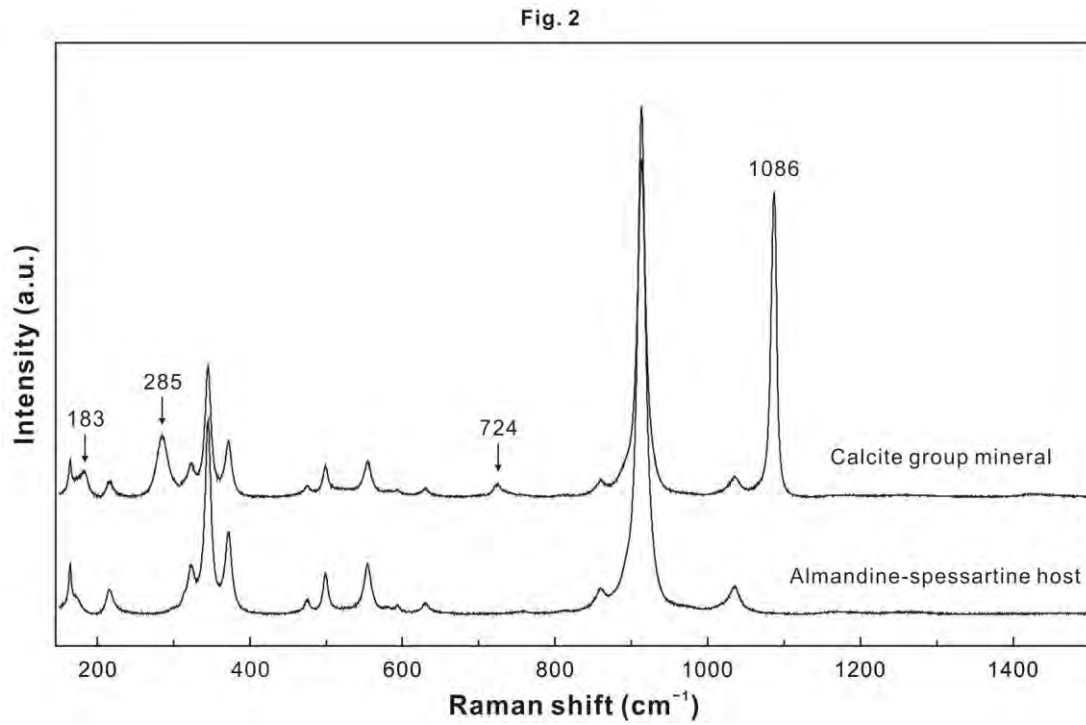
3

4

Fig. 3

5

6

Fig. 4

7

8

Fig. 5

9

10

Fig. 6

11

12